Southerly Winds Increase the Electricity Generated by Solar Photovoltaic Systems

Damon Waterworth[1] and Alona Armstrong[1.2]

[1]Lancaster Environment Centre, Lancaster University, Lancaster, LA1 4YQ, UK.

[2]Energy Lancaster, Lancaster University, Lancaster, LA1 4YF, UK.

Keywords: Solar energy, Wind Direction, Temperature, Solar park design, Panel orientation

Abstract

The urgent need to decarbonise energy supplies has prompted exponential growth of solar photovoltaic (PV) systems across the world. As the penetration of renewable energy sources increases, the need to accurately forecast electricity output heightens to ensure efficient energy system operation. While exposure to high temperatures and moisture are known to significantly reduce PV panel efficiency, the effects of wind on both PV panel temperature and electricity output are poorly resolved. Here, meteorological and PV panel production data from Westmill Solar Park, Oxfordshire, were examined to determine the influence of wind, cloud, ambient temperature and relative humidity. We found that, after solar radiation, relative humidity and cloud cover were the dominant controls of PV electricity output; increases in relative humidity and cloud cover were associated with decreased electricity outputs. However, when all other variables were held constant, the mean electricity generated under southerly winds was 20.4 – 42.9% greater than under northerly winds, with the difference greater at higher electricity outputs and attributable to differences in surface cooling capabilities caused by the PV array asymmetry. This finding suggests that PV electricity output predictions could be improved by incorporating wind direction into computer models. Moreover, there is potential to modify solar park design and deployment location to capitalise on wind benefits, especially in areas where panel temperatures are a leading cause of efficiency loss. Ensuring deployments are optimised for site environmental conditions could boost electricity outputs, and therefore profitability, with implications for system viability in post-subsidy markets.

1. Introduction

As the energy transition progresses and solar photovoltaics (PV) comprise an ever-larger share of the global energy portfolio it will become increasingly important to improve predictions of electricity output, especially for large, utility-scale ground-mounted systems (Bhandari *et al.,* 2015; Breyer *et al.,* 2017; Agoua *et al.,* 2018). Identifying and understanding the causes of meteorological sensitivity can improve energy predictions, negating the need for technological innovation and intermittency solutions (e.g. storage systems, demand-side management) to reduce power volatility and ensure electricity network resilience (Hanjalic *et al.,* 2007; Schiermeier, 2016; Gaglia *et al.,* 2017; Reindl *et al.,* 2017; Saffari *et al.,* 2018). Consequently, energy meteorology – where the grid utilises weather observations and machine learning techniques that predict renewable electricity outputs – has become increasingly pivotal in supporting industry decision-making and decarbonisation projects in both daily operations and long-term strategic planning (Traunmüller and Steinmaurer, 2010; Wan *et al.,* 2015; Reindl *et al.,* 2017; Agoua *et al.,* 2018; Ciriminna *et al.,* 2018). Moreover, improved understanding of meteorological-PV panel interactions

could be used within climate models to assess long-term risks to electricity supply given various climate change scenarios, and thus inform future energy system needs (Jerez *et al.,* 2015).

Whilst solar irradiance regulates PV panel electricity outputs, temperature is also influential as ambient temperature, solar absorption and electricity generation can cause the panel surface to heat up, resulting in reduced system efficiency (Armstrong and Hurley, 2010; Koehl *et al.,* 2011; Teo *et al.,* 2012; Kaldellis *et al.,* 2014; Gökmen *et al.,* 2016; Maghami *et al.,* 2016). Typically, a temperature increase of 1°C causes between a 0.14% and 0.47% reduction in relative efficiency, depending on the type of PV panel installed (Zaoui *et al.,* 2015; Cotfas *et al.,* 2018). PV panel temperature is also affected by wind and relative humidity, making predictions of electricity output relatively complex (Fesharaki *et al.,* 2011; Huld *et al.,* 2011; Kaplani and Kaplanis, 2014). For example, panels exposed to high winds undergo greater cooling via forced convective heat transfer to the ambient air (Tonui and Tripanagnostopoulos, 2007; Armstrong and Hurley, 2010; Schwingshackl *et al.,* 2013). By contrast, in low-wind, low-solar conditions (<4 ms^{-1}; <400 W/m^2), radiative cooling and natural convection (driven by temperature differences) prevail, and panel cooling reduces (Skoplaki and Palyvos, 2009; Huld *et al.,* 2011; Koehl *et al.,* 2011). This effect can be described using the linear function of the total in-plane irradiance with wind speed affecting the gradient of the slope (Koehl *et al.,* 2011). As such, given solar irradiance of 1000 W/m^2 and wind speeds of 1-2 ms^{-1}, the temperature difference between the ambient and PV panel is predicted to be ~32°C while winds of 9-10 ms^{-1} correspond with a temperature difference of just ~12°C (Koehl *et al.,* 2011).

Despite these observations wind speed and directional effects remain poorly resolved. Indeed, there is conflicting evidence on the value of incorporating wind into solar energy models. While studies such as Gaglia *et al.* (2017) claim that wind has a limited effect and thus can be disregarded, others (Koehl *et al.,* 2011; Schwingshackl *et al.,* 2013; An *et al.,* 2017) purport that the inclusion of wind speed significantly improves solar energy forecasting capabilities, particularly on very short time horizons (0 to 2 hours) which can see a 2% improvement in RMSE error (Agoua *et al.,* 2018). Equally, recent experimental models have shown that heat convection from the PV surface decreases when wind flows in parallel to the array, highlighting the potential importance of wind direction (Kaplani and Kaplanis, 2014). Nevertheless, findings are inconsistent and understanding limited due to the diverse range of environmental settings and panel types to be considered (e.g. Koehl *et al.,* 2011).

PV electricity output may also be substantially affected by changes in wind direction due to differences in the exposed surface area as described by Newton's Law of Cooling, which calculates the convection rate between an object and its surroundings (O'Sullivan, 1990; Vollmer, 2009; Teo *et al.,* 2012). As fixed-tilt ground-mounted solar arrays are generally orientated to maximise exposure to direct sunlight, in the northern (southern) hemisphere PV arrays are south (north) facing (Figure 1). Consequently, a greater proportion of the panel surface is exposed to southerly (northerly) winds compared to northerly (southerly) directions given the orientation and inclination (Tonui and Tripanagnostopoulos, 2007; Kaplani and Kaplanis, 2014). Thus, when all other factors are equal, the most efficient wind cooling should occur under southerly (northerly) winds (Jubayer *et al.,* 2016). Recent observations at Hadley Solar Park in England by Vasel and Iakovidis (2017) evidences this, reporting a power increase of up to 24% (300 kW) under southerly winds attributable to a 28% increase in convective heat transfer on the windward side of the solar array compared to the leeward side (e.g. Kaplani and Kaplanis, 2014; Jubayer *et al.,* 2016). However, it is likely that solar park design – the spacing of panel rows, height, and inclination – influence wind patterns including the levels of turbulence, with greater turbulence

increasing heat transfer and thus PV cooling and electricity output (Nickling, 1978; Iakovidis and Ting, 2014; Kaplani and Kaplanis, 2014; Iousef *et al.,* 2017).

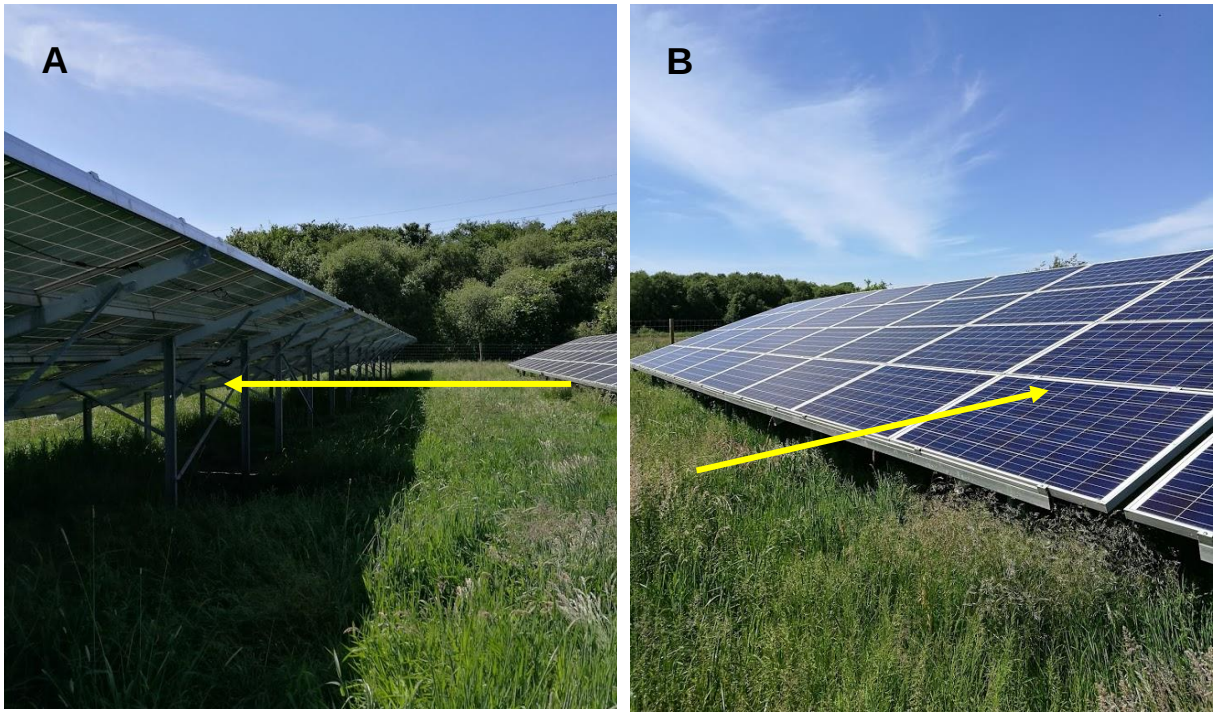

Figure 1: Visualisation of the (a) northerly and (b) southerly airstreams (arrows) under investigation. The front of the panel is sheltered from northerly winds but exposed to southerly winds, the situation is reversed for the back of the panel. Panels have a larger surface area exposed to the southerly winds given the skyward inclination.

As manufacturers usually provide static efficiency ratings based on standard test conditions (STCs), commonly at 25°C, 1000W/m^2 irradiance, and an airmass (AM) (direct optical path length) of 1.5, reliable energy predictions in response to changes in meteorological conditions is precluded (Bücher, 1997; Elibol *et al.,* 2017). Moreover, different design, technical characteristics and geographical contexts necessitate site-specific field testing to accurately predict electricity output (Mani and Pillai, 2010; Dubey *et al.,* 2013; Zaoui *et al.,* 2015; Gökmen *et al.,* 2016). For example, a recent study in Greece compared the PV efficiency reported in technical specifications (9.6% to 11.3%) with the actual efficiency observed at a solar park exposed to outdoor conditions. They observed average PV efficiencies 18% lower than those achieved in a controlled lab environment, as the prevailing weather conditions, namely high ambient temperature and solar radiation, lowered efficiencies by raising the panel temperature (Gaglia *et al.,* 2017).

Increased contributions from solar PV systems to electricity supply could be achieved through better predictions of electricity output. Whilst temperature effects are generally well resolved, developing models that incorporate wind speed and direction effects could offer useful insight and support energy grid operators in their efforts to achieve supply and demand equilibrium. Therefore, this paper aims to quantify the effects of wind and other meteorological variables on PV electricity output. It is hypothesised that: (1) wind will have the greatest influence after solar radiation and ambient temperature on the overall electricity output, and (2) solar panels will generate more electricity when winds originate from southerly

azimuths compared to northerly equivalents, with larger differences at higher wind speeds. These hypotheses will be tested using meteorological and PV array temperature and production data from a 5 MW ground-mounted solar park in the south of England. However, we also discuss implications for other localities and solar park site designs.

2. Materials and Methods

2.1 Study Area and Geographical Setting

This research was undertaken at Westmill Solar Park, Oxfordshire, UK (51°37'03''N, 01°38'45''W), which comprises 36 south-facing rows of fixed polycrystalline-silicon PV panels over 12.1 hectares of grassland. The PV array rows have a maximum height of 2.5 m, are 4.4 m wide, tilted due south at an angle of 30° and spaced 11.2 m from adjacent rows. The site has a rated capacity of 5 MW and a capacity factor of 12.3% based on 5,493 MWh of annual electricity generation between June 2013 and 2014. Like much of Western Europe, the area has a temperate oceanic climate (Köppen-Geiger classification) characterised by warm summers and mild winters (Geiger, 1954). The prevailing winds are westerly (Figure 2), which alternate warm tropical and cool polar maritime air masses, bringing inclement and humid weathers from the Atlantic Ocean (Met Office, 2018a). Rainfall is 685 mm per annum and partly cloudy skies are common (occurring >50% of the time) resulting in a high percentage of diffuse solar radiation and an average of 1632 hours of direct sunlight annually (1981 – 2010 reference period) – just 37% of the theoretical maximum daylight duration (Khademi *et al.,* 2016; Meteoblue, 2018a; Met Office, 2018b). Nevertheless, the potential yearly sum of global horizontal irradiation is among the highest on the UK mainland at ~1100-1150 kWh/m^2 (Šúri and Cebecauer, 2010).

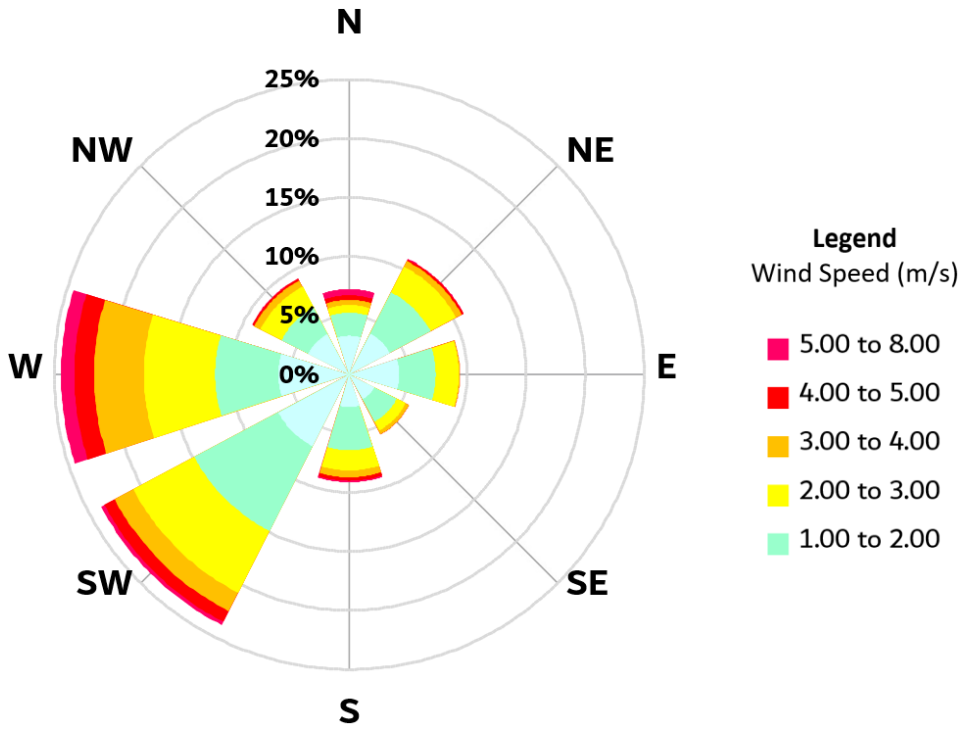

Mean wind speed:	1.6 m/s
Percent calm (< 0.3 m/s):	19.4%
Prevailing wind direction:	Westerly (24%)

Figure 2: Wind rose showing the percentage of wind hours from eight cardinal wind directions and their associated wind speeds. Observations are measured at a height of 1.5m above ground between June 27, 2013., 13:00 and June 27, 2014., 12:00 BST.

2.2 Data Sources, Preparation and Processing

Wind velocity (speed and direction), solar radiation (total and diffuse), ambient temperature and relative humidity, sampled every minute and averaged over hourly periods, were measured for a twelve month period from 27th June 2013 13:00 to 27th June 2014 12:00. Average ambient temperature (°C) and relative humidity (%) was derived from measurements taken using Tempcon HOBO data loggers (U30 model with S-THB-M002 sensor) at a height of 0.5 m above ground at four locations away from the photovoltaic panel rows. Total (global) and diffuse PAR (Photosynthetically Active Radiation) (J/m^2) was measured at one location (using the Delta-T BF5 sunshine recorder and GP1 data logger) at a height of 1.3 m. The diffuse fraction was used to estimate cloud cover given by the ratio of diffuse to total PAR (R_D/R_T) and used as a proxy for light intensity (on a scale from 0 to 1) whereby lower values indicate clearer sky conditions (Liu and Jordan, 1960; Roderick, 1999; Sağlam, 2010; Cruse *et al.,* 2015). Wind speed (ms^{-1}) and direction (°) were measured at the same logging station at 1.5 m above the surface using a three-cup anemometer (S-WSA-M003, S-WDA-M003 sensors). The site operator provided electricity output (kWh) and two sets of PV panel temperature (°C) readings, which were averaged for analysis.

All the data were recorded in British Summer Time (GMT+1) and quality controlled to eliminate blank fields and erroneous values. Only 'daytime' data was used in the analysis, classified as two hours after sunrise until two hours prior to sunset to account for rapid fluctuations following the National Oceanic and Atmospheric Administration algorithm (ESRL, 2014), resulting in 3848 usable time-series records. The data was split into northerly and southerly wind subsets whereby values between 95° and 265° were considered southerly and those between 0 and 85° and 275 and 360° northerly. The 10° buffer between the northerly and southerly groups recognises that wind direction is a fluctuating quantity which oscillates around its mean value (Sharples and Charlesworth, 1998). To isolate the influence of wind direction, all other meteorological variables were categorised following standard bin packing methodology (Cohen, 1992). First, the range was calculated for ambient temperature, relative humidity, wind speed, total and diffuse PAR data sets before the individual values were categorised into bins, informed by Sturge's Rule and the visual examination of histograms for each variable. Accordingly, ambient temperature, relative humidity and wind speed values were sorted into fourteen equal bin widths of 3°C, 5% and $0.5ms^{-1}$, respectively (Table 1). Due to the severely skewed data distribution, total and diffuse PAR were categorised into 5% segments so that there was an equal number of data points in each bin. Following, categorisation, northerly and southerly wind subsets were compared and paired if the bin codes for all corresponding variables (ambient temperature, wind speed, relative humidity, total and diffuse PAR) matched (see Appendix A for the full listing of southerly-northerly pairs). Multiple pairings were made when more than one northerly match was found for any given southerly data point.

Table 1: Bin packing of meteorological variables showing the minimum threshold value for each bin number. The 5% segmentation for global and diffuse PAR resulted in 228 data points per bin. For the full listing of southerly-northerly pairs see Appendix A.

Bin Number	Ambient Temperature (°C)	Relative Humidity (%)	Wind Speed (m/s)	Global PAR (J/m^2)	Diffuse PAR (J/m^2)
1	-6 – -3.1	30 – 34.9	0 – 0.4	1080 – 10500	2160 – 9898
2	-3 – -0.1	35 – 39.9	0.5 – 0.9	10501 – 39959	9899 – 39959
3	0 – 2.9	40 – 44.9	1 – 1.4	39960 – 86399	39960 – 78839
4	3 – 5.9	45 – 49.9	1.5 – 1.9	86400 – 140681	78840 – 123671
5	6 – 8.9	50 – 54.9	2 – 2.4	140682 – 203039	123672 – 166319
6	9 – 11.9	55 – 59.9	2.5 – 2.9	203040 – 258358	166320 – 204957
7	12 – 14.9	60 – 64.9	3 – 3.4	258359 – 331697	204958 – 239535
8	15 – 17.9	65 – 69.9	3.5 – 3.9	331698 – 401759	239536 – 279719
9	18 – 20.9	70 – 74.9	4 – 4.4	401760 – 480599	279720 – 324586
10	21 – 23.9	75 – 79.9	4.5 – 4.9	480600 – 557012	324587 – 366833
11	24 – 26.9	80 – 84.9	5 – 5.4	557013 – 646803	366834 – 421199
12	27 – 29.9	85 – 89.9	5.5 – 5.9	646804 – 750816	421200 – 477120
13	30 – 32.9	90 – 94.9	6 – 6.4	750817 – 871142	477121 – 534599
14	33 +	95 – 100	6.5 +	871143 – 999999	534600 – 613439
15				1000000 – 1199999	613440 – 693359
16				1200000 – 1499999	693360 – 784278
17				1500000 – 1799999	784279 – 884387
18				1800000 – 2099999	884388 – 999999
19				2100000 – 2599999	1000000 – 1299999
20				2600000 +	1300000 +

2.3 Statistical Methods

All statistical analyses were conducted using the open-source R programming software, version 3.4.3 (R Core Team, 2013), and significance determined at the 1% level ($p < 0.01$). Forward selection multiple regression was employed to test the first hypotheses, that wind will have the greatest influence after solar radiation and ambient temperature on the overall electricity output, using data when both solar elevation angle and electricity potential are highest – this solar noon (1300 BST, 365 data points in total) (ESRL, 2014) (Meyers *et al.,* 2016; Elibol *et al.,* 2017). Before conducting the multiple regression procedure, diagnostics plots provided checks for extreme values (Cook's distance), heteroscedasticity (Bartlett and Breusch-Pagan tests), and normality (Shapiro–Wilk test). Furthermore, individual variance inflation factors (VIF) were computed as an indicator of multicollinearity using the 'mctest' package to avoid overfitting (Faraway, 2016). Using the R 'scale' function, beta coefficients (reported in standard deviations between 0 and ±1) of the predictor variables were generated (based on the original multiple regression coefficients) to achieve a standardised solution enabling comparisons of the relative influence of the seven meteorological variables (Schroeder *et al.,* 2016). Akaike information criterion (AIC) (R: MASS package) was used to find the parsimonious model (Akaike, 1974). R^2 value was used to assess predictive power (Ranaboldo *et al.,* 2013; Schwingshackl *et al.,* 2013), and LMG scores (after authors: Lindeman, Merenda, and Gold, 1980) used to determine the relative hierarchy of predictor variables based on explanatory importance (Grömping, 2006; Grömping and Matthias, 2018). LMG scores were estimated using the 'calc.relimp' procedure in the 'relaimpo' package which gave the percentage of

variance contributed by each variable (Grömping, 2006). All LMG scores were normalised to 100% and calculated as a percentage of total R^2.

To test hypothesis two, that solar panels will generate more electricity when winds originate from southerly azimuths compared to northerly equivalents, with larger differences at higher wind speeds, a least squares linear regression model was fitted between northerly and southerly electricity output matches (Ranaboldo *et al.,* 2013). Linear regression was used to visualise the relationship between directional groups compared with the idealised one-to-one relationship expected if wind direction had no effect. Slopes, intercepts and confidence intervals were used to assess divergence from the one-to-one relationship and thus how the effect of wind direction changes as electricity output increases. Two further linear regression models were fitted between (1) wind speed and the electricity output difference (southerly minus northerly winds), and (2) panel temperature difference and electricity output difference, to determine whether wind cooling increased at higher wind speeds. A paired samples t-test was used to determine if there was a statistically significant difference in PV electricity output for northerly and southerly wind conditions, with electricity output readings logarithmically transformed ($\log_{10}$(value)) to satisfy the residual normality assumption but later back-transformed (antilog: 10^X) and the results reported in kWh (Kutner *et al.,* 2004; McDonald, 2009). This was achieved using five sub-sets of the data to determine the point of significance based on the following electricity output groups: all outputs, <50 kWh, >50 kWh, >100 kWh and >200 kWh.

3. Results

3.1 Meteorological controls over electricity output

The multiple regression model shows how each meteorological variable affected the observed PV electricity output. Relative humidity, cloud cover and diffuse PAR were significant controls, together explaining 66.3% of the variance in electricity produced ($F(3, 322)= 211$, $p <.001$), whereas wind speed, direction and ambient temperature were insignificant controls ($p > .05$) (Table 2). Cloud cover and relative humidity had the strongest influence over electricity output, together explaining 85% of the variance, with increases in both variables associated with decreases in electricity output (Table 2). By contrast, electricity output increased with diffuse PAR but was less influential, explaining only 15% of the variance (Table 2).

Table 2: Summary statistics of the dominant predictor variables as given by the regression model along with their LMG scores with 95% confidence limits. Residual standard error: 0.5834 on 322 degrees of freedom. $R^2 = 0.6628$, Adjusted $R^2 = 0.6597$. F-statistic: 211 on 3 and 322 DF, p-value: < 2.2e-16 ***, ns = no significance, * p < .05, *** p < .001.

~ Electricity output	**β Coefficient**	**Standard error**	**t value**	**Pr(>|t|)**	**Significance**	**LMG Score**
Intercept	3.816e-16	0.03231	0.000	1	ns	
Relative Humidity	-0.3328	0.04564	-7.292	2.38e-12	***	43% ± 7%
Cloud cover	-0.5153	0.0403	-12.788	< 2e-16	***	42% ± 6%
Diffuse PAR	0.2923	0.0415	7.042	1.15e-11	***	$15\%\ ^{+4\%}_{-6\%}$

3.2 Wind influences PV electricity output

The correlation between electricity output under northerly winds and electricity output under southerly winds has been plotted to demonstrate the effects of wind direction on PV electricity production. When there was no difference in electricity output for northerly and southerly wind matches, they fall on the one-to-one line. All points above this line indicate greater electricity production under northerly winds when compared to southerly equivalents, and visa-versa. Despite the insignificance of wind direction over PV electricity output when analysed with other meteorological variables (i.e. regression methods), the electricity output during northerly winds were, on average, only 73% of that during southerly winds conditions when all other variables (listed in Table 1) were held constant (Figure 3). However, there was a turning point in the data, with higher electricity outputs associated with northerly winds when total electricity generation was less than 50 kWh (Table 3). Moreover, the difference in mean electricity output between northerly and southerly wind groups increased significantly at higher PV electricity outputs: under southerly wind conditions electricity outputs were 23.8%, 27.8% and 42.9% higher at electricity outputs > 50, 100 and 200 kWh, respectively (Table 3).

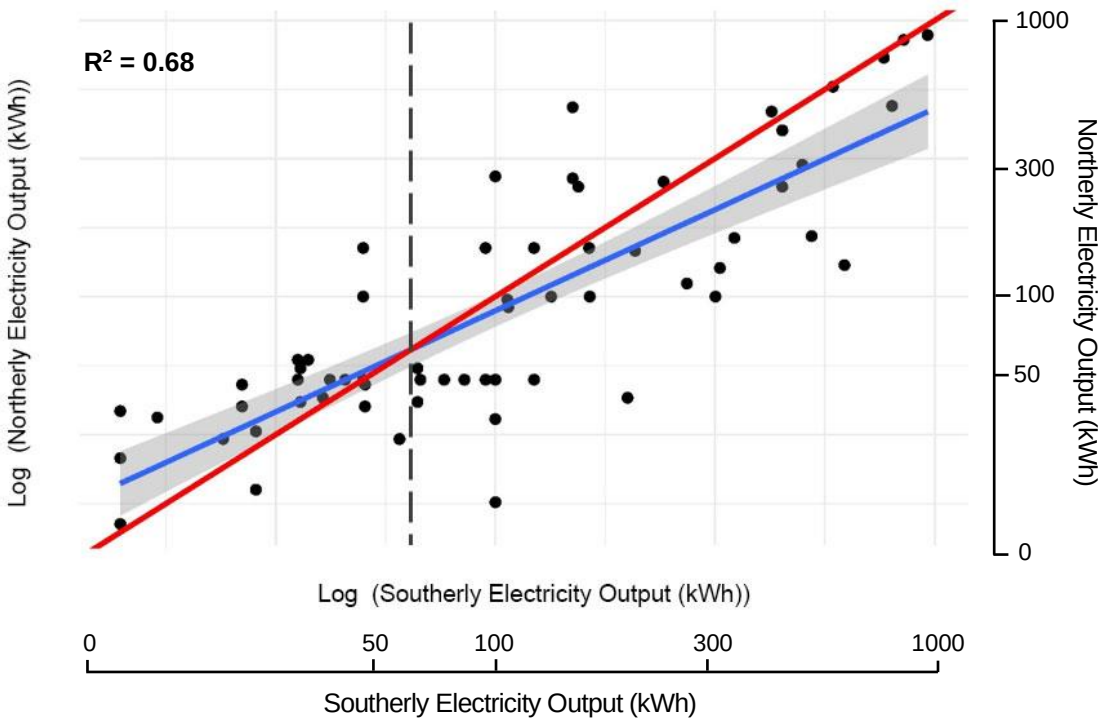

Figure 3: The relationship between electricity outputs during northerly and southerly winds. The blue line with the shaded area represents the trend of the observed electricity output (Y = 0.7325x + 0.4835) with 95% confidence limits. Points above (below) the 1:1 plot (red line) indicate where electricity output was higher when the wind was from the north (south). The vertical dashed line indicates the point where the trend changes from a northerly to southerly electricity surplus.

291

292 **Table 3**: The mean electricity output for northerly and southerly wind groups for each data subset. Means were back transformed by taking the antilog. SD =
293 Standard Deviation, DF = Degrees of Freedom, n = number of matches, : ns = no significance, * p < .01 and ** p < .001 = very significant).

		Northerly	**Southerly**	**South - North**		**Northerly**	**Southerly**			
Electricity	n	Mean (kWh)	Mean (kWh)	Difference (kWh)	DF	SD	SD	t-value	p-value	Significance
All outputs	70	147.5	177.6	30.1	69	0.42	0.47	1.5	0.149	ns
< 50 kWh	17	38.5	27.5	-11.0	16	0.17	0.17	4.3	< 0.001	**
> 50 kWh	53	181.8	225.1	43.3	52	0.42	0.4	2.9	0.005	*
> 100 kWh	32	260.0	332.2	72.2	31	0.42	0.32	3.1	0.004	*
> 200 kWh	18	344.4	492.0	147.6	17	0.37	0.21	4.3	< 0.001	**

294

Despite the significance of the relationship between wind direction and PV electricity output (Figure 3), differences in wind speed (R^2 = 0.02) and PV panel temperature (R^2 = 0.04) had no discernible effect on the observed power output difference between northerly and southerly wind matches (Figure 4).

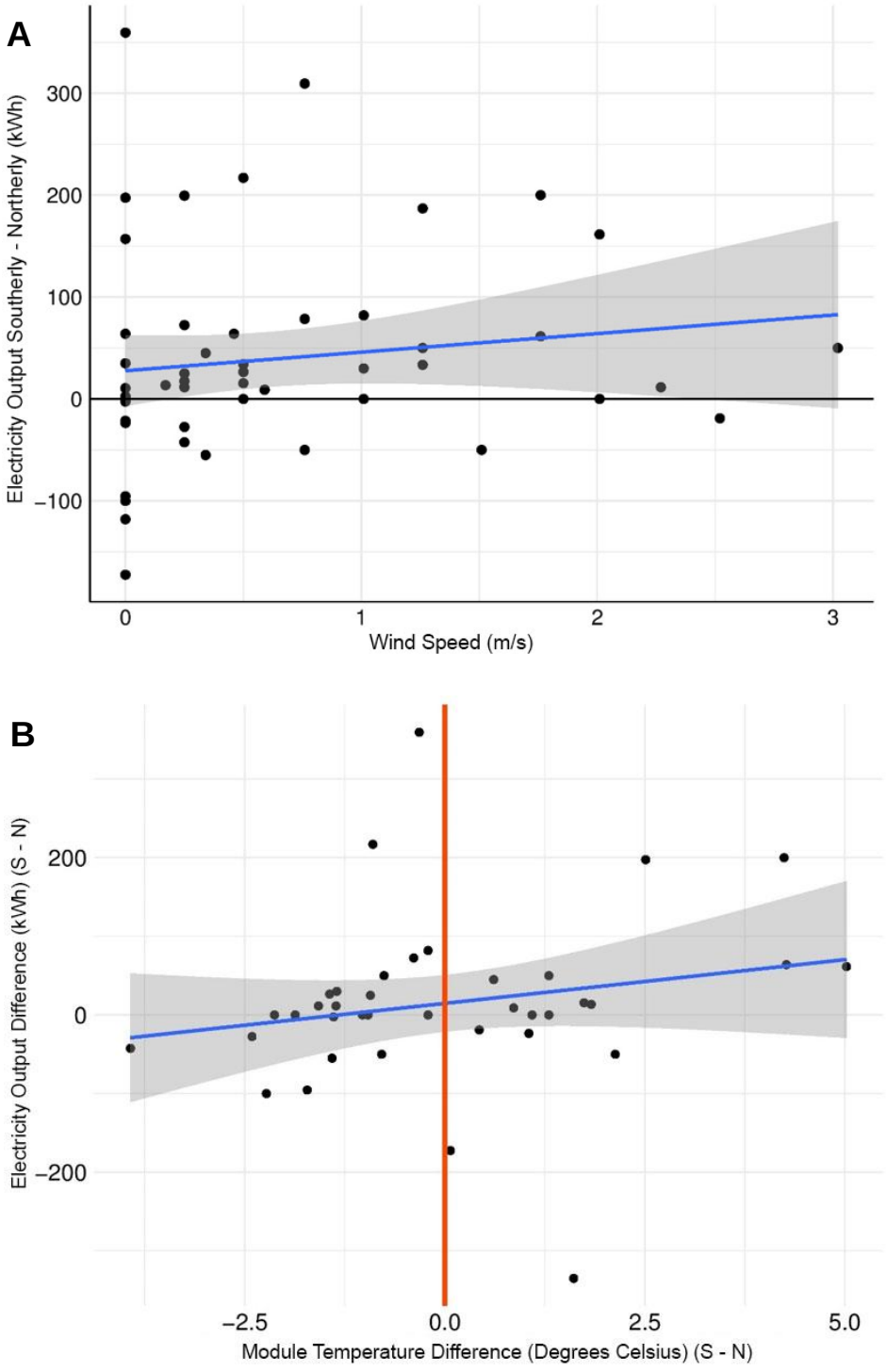

Figure 4: (a) The relationship between wind speed and electricity outputs (southerly minus northerly winds) when electricity output was > 50kWh with 95% confidence limits, and (b) the relationship between difference electricity output between southerly and northerly winds and panel temperature with 95% confidence limits.

4. Discussion

Improved predictions of PV electricity output would support the low-carbon energy transition by enabling grid stabilisation of intermittent electricity sources. Here, we show the influence of meteorological variables on electricity output, particularly how wind can affect the amount of electricity generated. Regarding energy and financial returns, electricity increases could make solar energy more attractive and competitive with fossil fuels, if wind cooling effects are utilised to the full extent.

4.1 Meteorological controls over PV electricity output

The hypothesis, that wind will have the greatest influence after solar radiation and ambient temperature on the overall electricity output, was rejected. Indeed, we found that ambient temperature, wind speed, and wind direction had no significant influence on electricity output whereas, cloud cover, relative humidity and diffuse PAR accounted for 43%, 42% and 15% of the variance in electricity output, respectively (Table 2). These findings are consistent with the environmental setting, supporting previous works in similarly humid, low wind speed and mild temperature environments (e.g. Gwandu and Creasey, 1995; Ghazi and Ip, 2014; Kazem and Chaichan, 2015; Khademi *et al.,* 2016). We found that PV sensitivity to cloud cover (-0.51) was greater than to relative humidity (-0.29) attributable to cloud formation and dissipation which causes frequent fluctuations in solar intensity and PV output in similar environments (Still *et al.,* 2009; Hill *et al.,* 2012; Challenge *et al.,* 2015). Indeed, passing clouds can shade panels and temporarily reduce electricity generation by 80% or more, exacerbating intermittency issues (Hanjalic *et al.,* 2007; Hill *et al.,* 2012; Khademi *et al.,* 2016; Bonkaney *et al.,* 2017; Reindl *et al.,* 2017; Touati *et al.,* 2017; Saffari *et al.,* 2018). In other climatic zones, the effects of clouds vary. For example, a field study in Brazil found that clouds are responsible for ~50% attenuation approximately 75% of the time, and in Niger, notable cloud impacts are limited to the short rainy season (Gu *et al.,* 2001; Bonkaney *et al.,* 2017). It is likely that the characteristically cloudy conditions at Westmill lead to diffuse PAR, as opposed to direct, being positively related to PV electricity output (Table 3): the relationship between diffuse PAR and PV electricity output is consistent with PV conversion theory (e.g. Iqbal, 1983; López and Batlles, 2004; Solanki, 2015).

The humid conditions (RH >70%) at Westmill Park likely had a more consistent adverse effect on electricity output, compared with cloud cover, creating a barrier of water vapor in front of the panel surface reducing the incidence of direct radiation available for electricity conversion (Iqbal, 1983; Gwandu and Creasey, 1995; Panjwani and Narejo, 2014). Further, there were occasions when the relative humidity reached 100% indicating that the dew point and ambient temperatures were equal. This caused the saturated air to periodically coat the panels in moisture thus increasing the reflectivity of the surface (optical refractive index) reducing the proportion of solar energy available for electricity generation. Whilst wind was not influential at Westmill, it may be in other climate zones, where substantial panel heat accumulation occurs, such as Qatar (Touati *et al.,* 2017). Here, temperature and humidity reduce the capacity for electrical conversion, while the wind transfers heat away from the panel surface, increasing system efficiency and electricity output (Touati *et al.,* 2017). Further, Westmill has relatively low wind speeds, limiting wind-induced cooling and drying compared to high-wind environments (e.g. 10 to 15 m/s) (Gökmen *et al.,* 2016; Jubayer *et al.,* 2016).

4.2 Wind influences PV electricity output

The hypothesis, that electricity output is increased under southerly winds, was supported, although no relationship with wind speed was found. Overall, northerly winds generated 73% of the electricity output of

southerly equivalents (Figure 3). This trend is attributable to the efficacy of wind cooling through convective heat transfer as described by Newton's Law of Cooling, whereby differences in exposed surface area likely resulted in differences in cooling rates between northerly and southerly directions and the solar park infrastructure (Cole and Sturrock, 1977; Keszthelyi *et al.,* 2003; Jubayer *et al.,* 2016; Goverde *et al.,* 2017; Lagouarde and Boulet, 2017). The southern face has a larger exposed surface area to maximise incident solar energy capture (Bardhi *et al.,* 2012; Teo *et al.,* 2012). By proxy, this means that panel exposure to southerly winds is greater than northerly equivalents, because the wind currents can pass more effectively over the length of the PV array on its southern side due to the skyward inclination. In contrast, northerly wind approaches result in mostly groundward deflection (Goverde *et al.,* 2017). This difference increases the potential for convective heat loss, and ultimately, improves surface cooling capabilities under southerly winds (Goverde *et al.,* 2017; Lagouarde and Boulet, 2017).

Differences in electricity output increased exponentially as the minimum electricity threshold was raised from 50 to 200 kWh, with southerly winds associated with electricity boosts between 20.4 and 42.9% (Table 2). This was likely caused by increased surface heating by solar absorption which increases the cooling benefits of wind when compared to instances of reduced solar absorption. Moreover, under southerly winds, return flows can be generated when intercepted by the panels, augmenting cooling on the north-facing underside of the panels (Goverde *et al.,* 2017). Specifically, turbulent eddies form in the wake of the array (gap areas) and a return flow is generated which cools the underside of the array structure (Figure 5). Conversely, equivalent northerly winds are unlikely to induce counterflow cooling on the southern side due to the skyward tilt. This is because arrays under northerly winds act as a shelterbelt (or wind block) (Sharples and Charlesworth, 1998), creating areas of low wind speed adjacent to the southern edge – a phenomenon associated with many natural and human elements including hedges (e.g. Wilson and Yee, 2003; Stull, 2012) and buildings (e.g. Oke, 1988). Nonetheless, for both northerly and southerly winds, air passes beneath the array and accelerates due to the venturi effect, resulting in micro-pressure changes drawing air currents toward the base of the array structure (Figure 5).

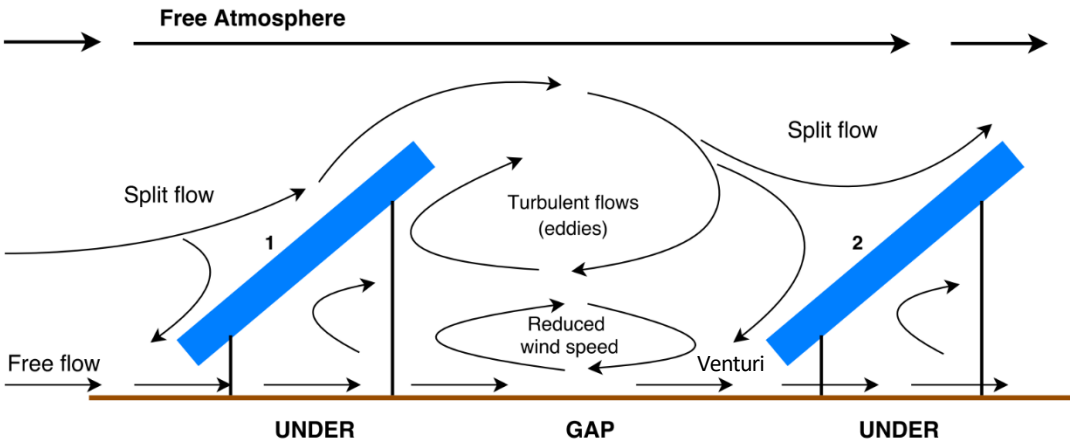

Figure 5: A schematic of wind flows at a theoretical solar park (cross-section view looking west) given a wake interference landscape and southerly wind scenario (Northern Hemisphere) (after Gandemer 1976; Kovar-Panskus et al., 2002). Markers 1 and 2 indicate stagnation points.

For electricity outputs <50 kWh the opposite trend was found; northerly winds resulted in significantly higher electricity output than southerly equivelents (Figure 3). This reversal in trend may be attributed to greater boundary layer heat exchange driven by increased turbulent airflow under northerly winds (Bogren *et al.,* 2001; Goverde *et al.,*

2017; Marinić-Kragić *et al.,* 2018). Since solar arrays are asymmetrical, turbulence intensity is contingent on array orientation and the prevailing wind direction (e.g. Cole and Sturrock, 1977; Jubayer and Hangan, 2012). Given southerly winds, panel surfaces affect air currents in similar ways to pitched roofs, deflecting wind upwards and along the length of the structure (Sharples and Charlesworth, 1998). This encourages laminar flows, restricting heat loss by creating an insulation layer that restricts mixing (Jubayer and Hangan, 2012; Stull, 2012; Goverde *et al.,* 2017). Conversely, when winds approach the northern, downward facing edge, turbulence was likely increased, breaking up the laminar layers, increasing turbulence and thereby boundary layer heat exchange (Goverde *et al.,* 2017). This effect is supported by wind tunnel experiments, for example increases in turbulence intensity from 0.5% (near laminar) to 12% has been shown to increase the PV heat flux to the ambient air by ~40% (Iakovidis and Ting, 2014). At greater electricity outputs the impact of turbulence is likely subsumed by other factors such as resistive ('Joule') and solar heating effects.

Despite the differences in electricity outputs with wind direction, PV panel temperatures were not affected (Figure 5). This was not expected and contradictory to the understanding that lower panel temperatures result in greater electricity outputs. Further, it is counterintuitive given wind flow is the primary cooling mechanism governing the efficiency of PV systems (Xydis, 2013; Jubayer *et al.,* 2016; Vasel and Iakovidis, 2017; Wu *et al.,* 2017; Styszko *et al.,* 2018). Perhaps because solar energy in not entirely converted to electricity, the Joule effect – where waste heat is generated during the light-to-electricity conversion process – offset the initial cooling attributable to surface winds, initiating a stabilising feedback loop (Armstrong and Harley, 2010; Morchid and Conlon, n.d.) (Figure 6). Conversely, less wind cooling under northerly winds reduces electricity, Joule heating and temperature implications throughout the cycle, initiating a similar stabilising effect (Figure 6).

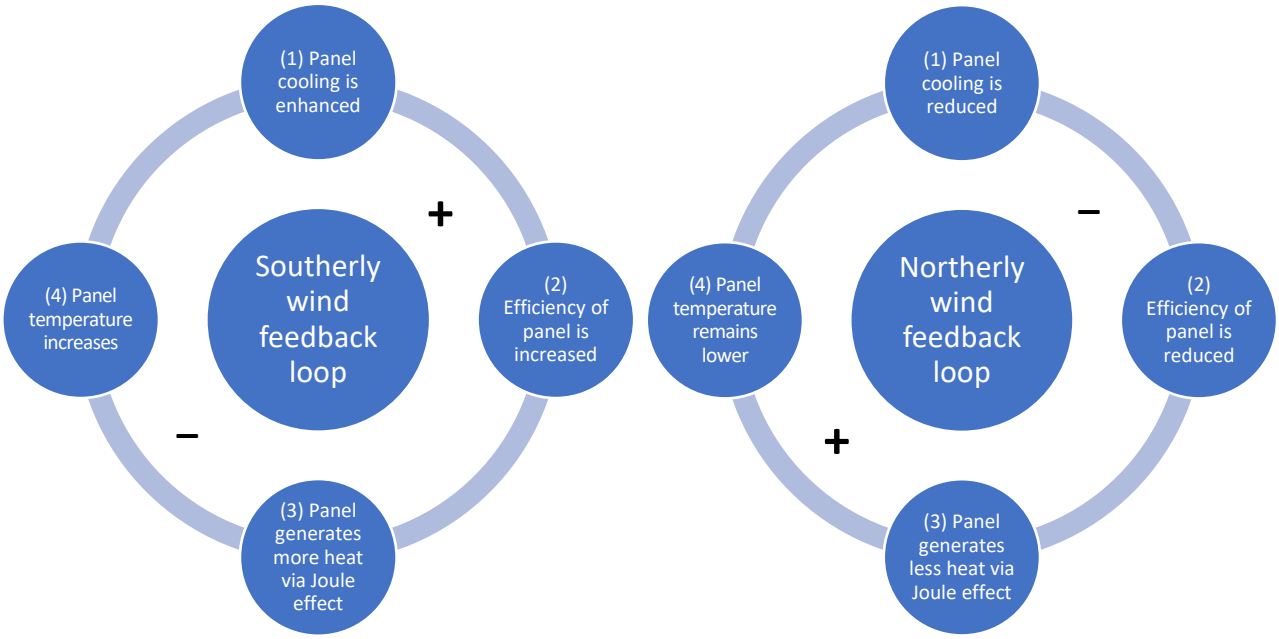

Figure 6: Hypothesised southerly and northerly wind feedback loops that explain the observed similarities in panel temperatures but differences in electricity output.

These hypothesised feedback loops are supported by consideration of heat transfers (Figure 8). Shortwave radiation from the sun (Q_{rad}) and resistive (Joule) effects associated with electricity generation create heat while electricity generation (P_{pv}), natural and forced convection (Q_{conv}) dispel heat from panels. Under calm winds, natural convection prevails, caused by thermal differences between the hotter PV panel surface (T_{pv}) and cooler ambient air (T_a), whereas stronger winds associate with forced convection, usually a more effective means of heat transfer (Keszthelyi *et al.,* 2003; Skoplaki and Palyvos, 2009; Huld *et al.,* 2011; Koehl *et al.,* 2011; Goverde *et al.,* 2017; Lagouarde and Boulet, 2017). The results from this study (Figure 5) imply that heat loss through convective transfer (sum of both natural and forced components) was approximately proportional to the heat accumulated through absorption of shortwave radiation (Q_{rad}) and Joule effects under southerly winds. Heat losses (P_{pv} , natural and forced convection) were not sufficient to overcome the heat generated (from the absorbed solar radiation and Joule effects) due to the prevalence of low wind (<3 m/s), low solar conditions (Figure 5) and thus the limited wind cooling benefits associated with forced convection (Skoplaki and Palyvos, 2009; Huld *et al.,* 2011; Koehl *et al.,* 2011). However, at higher electricity outputs, these same causes of heat loss likely overwhelmed any heat generated leading to a significant surplus in electricity output of up to 42.9% under southerly winds (Table 3). This is substantially greater than the 24% (300 kW) increase in peak power observed in a similar study at Hadley solar farm, UK (Vasel and Iakovidis, 2017).

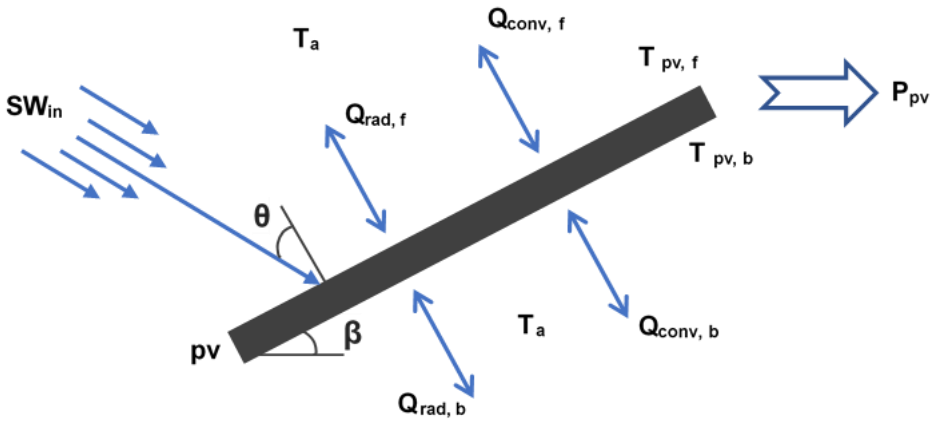

Figure 7: Schematic of heat exchanges, radiation (Q_{rad}) and convection (Q_{conv}) at the front (f) and back (b) of the solar panel (pv). P_{pv} relates to the electricity generated, T_a and T_{pv} are the ambient and panel temperatures, respectively. β and θ are the panel inclination angle and incoming direct solar energy component (SW_{in}), respectively (after Bardhi *et al.,* 2012).

4.3 Further research and implications for solar park innovations

In order to capitalise on the influence of meteorological conditions on solar park electricity outputs across the world, a combination of further field research, controlled experimentation of the independent variables and modelling approaches is required. Wind characteristics and associated cooling benefits vary considerably across different locations. At Westmill, prevailing westerly and south-westerly winds complement southerly facing panels, providing natural cooling. However, in the sunbelt (0 to 40°N) where annual global irradiance is double that of Westmill (~2000 - 2500 kWh/m^2) and ambient temperatures often exceed 30°C (Šúri and Cebecauer, 2010; Kawajiri *et al.,* 2011), north-east trade winds (e.g. Qatar: Meteoblue, 2018b) are unlikely to be as effective at cooling panels with a southerly orientation given the sheltering effect (Sharples and Charlesworth, 1998).

Moreover, as global circulation patterns follow changes in the suns position, seasonal shifts in wind direction may impact panel productivity differently according to the time of year. These aspects highlight the location-specific nature of meteorological interactions, as such developers must effectively harmonise panel efficiency and solar insolation receipts to locate the best sites (Bhandari *et al.,* 2015).

Field studies like this one are highly location specific reflecting the unique characteristics (e.g. climatological, technical, site management) that influence PV performance. In order to capitalise on these findings, and improve the efficiency of future solar parks, it would be valuable to investigate how differences in panel inclination, orientation, type, spacing and location affect the balance of heat sources and sinks through changes in turbulence, conduction and exposure. There is some existing understanding, for example, changes in park design, specifically orientation, have been found to provide an electricity boost at little or no additional expense (Cheng and Hammond, 2017). Further, wind tunnel simulations (e.g. Goverde *et al.,* 2017) and microclimate studies (e.g. Fthenakis and Yu, 2013) have demonstrated that forced airflows over the panel surface transports heat downwind. As such, arrays furthest downwind experience restricted heat transfer capabilities (natural convection) when compared to those upstream, as the panel-ambient temperature difference is reduced (Ali *et al.,* 2017; Goverde *et al.,* 2017) suggesting that the most efficient solar park site designs will be those with the smallest number of rows aligned with the dominant wind direction. Finally, panel interactions reduce the average wind speed such that northernmost panels have reduced cooling benefits (via forced convection) under southerly airstreams (Fthenakis and Yu, 2013). As southerly winds significantly increase electricity output, solar parks elongated along the west-east axis may be able to capitalise on increased wind exposure by reducing the north-south distance and the proportion of panels subjected to an artificially warmed airflow (Fthenakis and Yu, 2013; Ali *et al.,* 2017; Goverde *et al.,* 2017).

5.0. Conclusion

Solar PV is an integral part of national and global decarbonisation strategies, with growth accelerating as costs decline. As the penetration of solar PV grows, it is becoming increasingly valuable to be able to improve predictions of electricity generation, including the impact of local meteorological conditions. We found that the electricity output at Westmill Solar Park was primarily influenced by humidity and cloud cover with diffuse PAR important but less influential; together humidity, cloud cover and diffuse PAR explained 66% of the variance in electricity output. Wind direction, but not speed, was also found to significantly influence electricity generation. On average electricity outputs when the wind originated from the north were only 73% of outputs when wind was from the south. At the highest electricity outputs, 42.9% (147.6 kWh) more electricity was produced under southerly winds compared to northerly equivalents. These differences associated with wind direction are attributable to changes in the balance of heat generated and lost, which relate to the surface geometry, the role of turbulence, and PV array spacing. These findings could inform both solar park location and design decisions, if this understanding was extended across different climatic regions and solar park designs. Ultimately, improved understanding of the effect of meteorology on PV electricity generation will improve grid management and the profitability of this rapidly accelerating means of low carbon electricity production.

Acknowledgments

We thank Adam Twine and Westmill Solar Park for providing site access and Westmill Solar Cooperative Limited for the production and PV module temperature data. Dr Alona Armstrong acknowledges financial support from an Energy Lancaster Fellowship, a Lancaster University Early Career Small Grant a NERC Industrial Innovation Fellowship (NE/R013489/1).

References

[1] Agoua, X.G., Girard, R. and Kariniotakis, G., 2018. Short-term spatio-temporal forecasting of photovoltaic power production. *IEEE Transactions on Sustainable Energy*, *9*(2), pp.538-546.

[2] Akaike, H., 1974. A new look at the statistical model identification. *IEEE transactions on automatic control*, *19*(6), pp.716-723.

[3] Ali, M., Iqbal, M.H., Sheikh, N.A., Ali, H.M., Shehryar Manzoor, M., Khan, M.M. and Tamrin, K.F., 2017. Performance Investigation of Air Velocity Effects on PV Modules under Controlled Conditions. *International Journal of Photoenergy*, *2017*.

[4] An, D.S., Poudel, P., Bae, S.H., Park, K.W. and Jang, B., 2017. Improved Photovoltaic MATLAB Modeling Accuracy by Adding Wind Speed Effect. *조선자연과학논문집*, *10* (1), pp.58-63.

[5] Armstrong, S. and Hurley, W.G., 2010. A thermal model for photovoltaic panels under varying atmospheric conditions. *Applied Thermal Engineering*, *30*(11-12), pp.1488-1495.

[6] Bardhi, M., Grandi, G. and Tina, G.M., 2012, March. Comparison of PV cell temperature estimation by different thermal power exchange calculation methods. In *Proceedings of the International Conference on Renewable Energies and Power Quality (ICREPQ'12), Santiago de Compostela, Spain* (pp. 28-30).

[7] Bhandari, K.P., Collier, J.M., Ellingson, R.J. and Apul, D.S., 2015. Energy payback time (EPBT) and energy return on energy invested (EROI) of solar photovoltaic systems: A systematic review and meta-analysis. *Renewable and Sustainable Energy Reviews*, *47*, pp.133-141.

[8] Bogren, J., Gustavsson, T. and Karlsson, M., 2001. Temperature differences in the air layer close to a road surface. *Meteorological Applications, 8(4), pp.385-395.*

[9] Bonkaney, A.L., Saidou, M. and Adamou, R., 2017. Impact of Climatic Parameters on the Performance of Solar Photovoltaic (PV) Module in Niamey. *Smart Grid and Renewable Energy*, *8* (12), p.379.

[10] Breyer, C., Bogdanov, D., Aghahosseini, A., Gulagi, A., Child, M., Oyewo, A.S., Farfan, J., Sadovskaia, K. and Vainikka, P., 2017. Solar photovoltaics demand for the global energy transition in the power sector. *Progress in Photovoltaics: Research and Applications*.

[11] Bücher, K., 1997. Site dependence of the energy collection of PV modules. *Solar Energy Materials and Solar Cells*, *47*(1-4), pp.85-94.

[12] Challenge, S., Gordo, E., Khalaf, N., Strangeowl, T., Dolino, R. and Bennett, N., 2015. Factors Affecting Solar Power Production Efficiency.

[13] Cheng, V.K. and Hammond, G.P., 2017. Life-cycle energy densities and land-take requirements of various power generators: A UK perspective. *Journal of the Energy Institute*, *90*(2), pp.201-213.

[14] Ciriminna, R., Albanese, L., Meneguzzo, F. and Pagliaro, M., 2018. New energy and weather services in the context of the energy transition. *Energy Technology*, *6*(1), pp.134-139.

[15] Cohen, J., 1992. A power primer. *Psychological bulletin*, *112* (1), p.155-159.

[16] Cole, R.J. and Sturrock, N.S., 1977. The convective heat exchange at the external surface of buildings. *Building and Environment*, *12*(4), pp.207-214.

[17] Cotfas, D.T., Cotfas, P.A. and Machidon, O.M., 2018. Study of Temperature Coefficients for Parameters of Photovoltaic Cells. *International Journal of Photoenergy*, *2018*.

[18] Cruse, M.J., Kucharik, C.J. and Norman, J.M., 2015. Using a simple apparatus to measure direct and diffuse photosynthetically active radiation at remote locations. *PloS one*, *10*(2), p.e0115633.

[19] Dubey, S., Sarvaiya, J.N. and Seshadri, B., 2013. Temperature dependent photovoltaic (PV) efficiency and its effect on PV production in the world–a review. *Energy Procedia*, *33*, pp.311-321.

[20] Elibol, E., Özmen, Ö.T., Tutkun, N. and Köysal, O., 2017. Outdoor performance analysis of different PV panel types. *Renewable and Sustainable Energy Reviews*, *67*, pp.651-661.

[21] ESRL, 2014. NOAA Solar Calculations details. [ONLINE] Available at: https://esrl.noaa.gov/gmd/grad/solcalc/calcdetails.html [Accessed: 5 May 2018].

[22] Faraway, J.J., 2016. *Extending the linear model with R: generalized linear, mixed effects and nonparametric regression models* (Vol. 124). CRC press.

[23] Fesharaki, V.J., Dehghani, M., Fesharaki, J.J. and Tavasoli, H., 2011, November. The effect of temperature on photovoltaic cell efficiency. In *Proceedings of the 1st International Conference on Emerging Trends in Energy Conservation–ETEC, Tehran, Iran* (pp. 20-21).

[24] Fthenakis, V. and Yu, Y., 2013. Analysis of the potential for a heat island effect in large solar farms. In *Photovoltaic Specialists Conference (PVSC), 2013 IEEE 39th* (pp. 3362-3366). IEEE.

[25] Gaglia, A.G., Lykoudis, S., Argiriou, A.A., Balaras, C.A. and Dialynas, E., 2017. Energy efficiency of PV panels under real outdoor conditions–An experimental assessment in Athens, Greece. *Renewable Energy*, *101*, pp.236-243.

[26] Gandemer, J., 1976. *Intégration du phénomène vent dans la conception du milieu bâti: guide méthodologique et conseils pratiques*. Secrétariat Général du Groupe Central des Villes Nouvelles.

[27] Geiger, R., 1954. Landolt-Börnstein–Zahlenwerte und Funktionen aus Physik, Chemie, Astronomie, Geophysik und Technik, alte Serie Vol. 3. *Ch. Klassifikation der Klimate nach W. Köppen.–Springer, Berlin*, pp.603-607.

[28] Ghazi, S. and Ip, K., 2014. The effect of weather conditions on the efficiency of PV panels in the southeast of UK. *Renewable Energy*, *69*, pp.50-59.

[29] Gökmen, N., Hu, W., Hou, P., Chen, Z., Sera, D. and Spataru, S., 2016. Investigation of wind speed cooling effect on PV panels in windy locations. *Renewable Energy*, *90*, pp.283-290.

[30] Goverde, H., Goossens, D., Govaerts, J., Catthoor, F., Baert, K., Poortmans, J. and Driesen, J., 2017. Spatial and temporal analysis of wind effects on PV modules: Consequences for electrical power evaluation. *Solar Energy*, *147*, pp.292-299.

[31] Grömping, U., 2006. Relative importance for linear regression in R: the package relaimpo. *Journal of statistical software*, *17*(1), pp.1-27.

[32] Grömping, U. and Matthias, L., 2018. Package 'relaimpo'.

[33] Gu, L., Fuentes, J.D., Garstang, M., da Silva, J.T., Heitz, R., Sigler, J. and Shugart, H.H., 2001. Cloud modulation of surface solar irradiance at a pasture site in southern Brazil. *Agricultural and Forest Meteorology*, *106*(2), pp.117-129.

[34] Gwandu, B.A.L. and Creasey, D.J., 1995. Humidity: a factor in the appropriate positioning of a photovoltaic power station. *Renewable Energy*, *6*(3), pp.313-316.

[35] Hanjalic, K., van de Krol, R. and Lekic, A. eds., 2007. *Sustainable energy technologies: options and prospects*. Springer Science & Business Media.

[36] Hill, C.A., Such, M.C., Chen, D., Gonzalez, J. and Grady, W.M., 2012. Battery energy storage for enabling integration of distributed solar power generation. *IEEE Transactions on smart grid*, *3*(2), pp.850-857.

[37] Huld, T., Friesen, G., Skoczek, A., Kenny, R.P., Sample, T., Field, M. and Dunlop, E.D., 2011. A power-rating model for crystalline silicon PV modules. *Solar Energy Materials and Solar Cells*, *95* (12), pp.3359-3369.

[38] Iakovidis, F. and Ting, D.S.K., 2014, November. Effect of Free Stream Turbulence on Air Cooling of a Surrogate PV Panel. In *ASME 2014 International Mechanical Engineering Congress and Exposition* (pp. V06BT07A001-V06BT07A001). American Society of Mechanical Engineers.

[39] Iousef, S., Montazeri, H., Blocken, B. and Van Wesemael, P.J.V., 2017. On the use of non-conformal grids for economic LES of wind flow and convective heat transfer for a wall-mounted cube. *Building and Environment*, *119*, pp.44-61.

[40] Iqbal, M., 1983. An introduction to solar radiation.

[41] Jerez, S., Tobin, I., Vautard, R., Montávez, J.P., López-Romero, J.M., Thais, F., Bartok, B., Christensen, O.B., Colette, A., Déqué, M. and Nikulin, G., 2015. The impact of climate change on photovoltaic power generation in Europe. *Nature communications*, *6*, p.10014.

[42] Jubayer, C.M. and Hangan, H., 2012. Wind effects on photovoltaic (PV) panels–A CFD approach. *The Wind Engineering, Energy and Environment (WindEEE) Research Institute, Western University, London, ON*.

[43] Jubayer, C.M., Siddiqui, K. and Hangan, H., 2016. CFD analysis of convective heat transfer from ground mounted solar panels. *Solar Energy*, *133*, pp.556-566.

[44] Kaldellis, J.K., Kapsali, M. and Kavadias, K.A., 2014. Temperature and wind speed impact on the efficiency of PV installations. Experience obtained from outdoor measurements in Greece. *Renewable Energy*, *66*, pp.612-624.

[45] Kaplani, E. and Kaplanis, S., 2014. Thermal modelling and experimental assessment of the dependence of PV module temperature on wind velocity and direction, module orientation and inclination. *Solar Energy*, *107*, pp.443-460.

[46] Kawajiri, K., Oozeki, T. and Genchi, Y., 2011. Effect of temperature on PV potential in the world. *Environmental science & technology*, *45*(20), pp.9030-9035.

[47] Kazem, H.A. and Chaichan, M.T., 2015. Effect of humidity on photovoltaic performance based on experimental study. *International Journal of Applied Engineering Research (IJAER)*, *10* (23), pp.43572-43577.

[48] Keszthelyi, L., Harris, A.J. and Dehn, J., 2003. Observations of the effect of wind on the cooling of active lava flows. *Geophysical Research Letters*, *30*(19).

[49] Khademi, M., Moadel, M. and Khosravi, A., 2016. Power prediction and technoeconomic analysis of a solar PV power plant by MLP-ABC and COMFAR III, considering cloudy weather conditions. *International Journal of Chemical Engineering*, *2016*.

[50] Koehl, M., Heck, M., Wiesmeier, S. and Wirth, J., 2011. Modelling of the nominal operating cell temperature based on outdoor weathering. *Solar Energy Materials and Solar Cells*, *95*(7), pp.1638-1646.

[51] Kovar-Panskus, A., Louka, P., Sini, J.F., Savory, E., Czech, M., Abdelqari, A., Mestayer, P.G. and Toy, N., 2002. Influence of geometry on the mean flow within urban street canyons–a comparison of wind tunnel experiments and numerical simulations. *Water, Air, & Soil Pollution: Focus*, *2*(5), pp.365-380.

[52] Kutner, M.H., Nachtsheim, C. and Neter, J., 2004. *Applied linear regression models*. McGraw-Hill/Irwin.

[53] Lagouarde, J.P. and Boulet, G., 2017. Energy balance of continental surfaces and the use of surface temperature. In *Land Surface Remote Sensing in Continental Hydrology* (pp. 323-361).

[54] Lindeman, R.H., Merenda, P.F. and Gold, R.Z., 1980. *Introduction to bivariate and multivariate analysis* (No. 04; QA278, L553.). Glenview, IL: Scott, Foresman.

[55] Liu, B.Y. and Jordan, R.C., 1960. The interrelationship and characteristic distribution of direct, diffuse and total solar radiation. *Solar energy*, *4* (3), pp.1-19.

[56] López, G. and Batlles, F.J., 2004, September. Estimate of the atmospheric turbidity from three broad-band solar radiation algorithms. A comparative study. In *Annales Geophysicae*(Vol. 22, No. 8, pp. 2657-2668).

[57] Maghami, M.R., Hizam, H., Gomes, C., Radzi, M.A., Rezadad, M.I. and Hajighorbani, S., 2016. Power loss due to soiling on solar panel: A review. *Renewable and Sustainable Energy Reviews*, *59*, pp.1307-1316.

[58] Mani, M. and Pillai, R., 2010. Impact of dust on solar photovoltaic (PV) performance: Research status, challenges and recommendations. *Renewable and Sustainable Energy Reviews*, *14*(9), pp.3124-3131.

[59] Marinić-Kragić, I., Nižetić, S., Grubišić-Čabo, F. and Papadopoulos, A.M., 2018. Analysis of flow separation effect in the case of the free-standing photovoltaic panel exposed to various operating conditions. *Journal of cleaner production*, *174*, pp.53-64.

[60] McDonald, J.H., 2009. Handbook of Biological Statistics (Vol. 2). Baltimore, MD: Sparky House Publishing.

[61] Meteoblue, 2018a. Climate Brize Norton: *Cloudy, sunny and precipitation days.* [ONLINE] Available at: https://www.meteoblue.com/en/weather/forecast/modelclimate/brize-norton_united-kingdom_2654659 [Accessed: 5 June 2018].

[62] Meteoblue, 2018b. Climate Doha: *Cloudy, sunny and precipitation days.* [ONLINE] Available at: https://www.meteoblue.com/en/weather/forecast/modelclimate/doha_qatar_290030 [Accessed: 15 August 2018].

[63] Met Office, 2018a. Air mass types. [ONLINE] Available at: https://www.metoffice.gov.uk/learning/atmosphere/air-masses/types [Accessed: 25 June 2018].

[64] Met Office, 2018b. Brize Norton climate averages 1981 to 2010. [ONLINE] Available at: https://www.metoffice.gov.uk/public/weather/climate/gcnyknk2h [Accessed: 5 June 2018].

[65] Meyers, L.S., Gamst, G. and Guarino, A.J., 2016. *Applied multivariate research: Design and interpretation*. Sage publications.

[66] Morchid, H. and Conlon, M., n.d. Investigation of the effects of Joule heating on the performance of photovoltaic modules.

[67] Oke, T.R., 1988. Street design and urban canopy layer climate. *Energy and buildings*, *11*(1-3), pp.103-113.

[68] O'Sullivan, C.T., 1990. Newton's law of cooling—a critical assessment. *American Journal of Physics*, *58* (10), pp.956-960.

[69] Panjwani, M.K. and Narejo, G.B., 2014. Effect of humidity on the efficiency of solar cell (photovoltaic). *International Journal of Engineering Research and General Science*, *2*(4), pp.499-503.

[70] R Core Team, 2013. R: A language and environment for statistical computing. *R Foundation for Statistical Computing*, *Vienna, Austria.* http://www.r-project.org/

[71] Ranaboldo, M., Giebel, G. and Codina, B., 2013. Implementation of a Model Output Statistics based on meteorological variable screening for short-term wind power forecast. *Wind Energy*, *16*(6), pp.811-826.

[72] Reindl, T., Walsh, W., Yanqin, Z. and Bieri, M., 2017. Energy meteorology for accurate forecasting of PV power output on different time horizons. *Energy Procedia*, *130*, pp.130-138.

[73] Roderick, M.L., 1999. Estimating the diffuse component from daily and monthly measurements of global radiation. *Agricultural and Forest Meteorology*, *95* (3), pp.169-185.

[74] Saffari, M., de Gracia, A., Fernández, C., Belusko, M., Boer, D. and Cabeza, L.F., 2018. Optimized demand side management (DSM) of peak electricity demand by coupling low temperature thermal energy storage (TES) and solar PV. *Applied Energy*, *211*, pp.604-616.

[75] Sağlam, Ş., 2010. Meteorological parameters effects on solar energy power generation. *WSEAS Transactions on Circuits and Systems*, *9*(10), pp.637-649.

[76] Schroeder, L.D., Sjoquist, D.L. and Stephan, P.E., 2016. *Understanding regression analysis: An introductory guide* (Vol. 57). Sage Publications.

[77] Schwingshackl, C., Petitta, M., Wagner, J.E., Belluardo, G., Moser, D., Castelli, M., Zebisch, M. and Tetzlaff, A., 2013. Wind effect on PV module temperature: Analysis of different techniques for an accurate estimation. *Energy Procedia*, *40*, pp.77-86.

[78] Sharples, S. and Charlesworth, P.S., 1998. Full-scale measurements of wind-induced convective heat transfer from a roof-mounted flat plate solar collector. *Solar Energy*, *62*(2), pp.69-77.

[79] Skoplaki, E. and Palyvos, J.A., 2009. On the temperature dependence of photovoltaic module electrical performance: A review of efficiency/power correlations. *Solar energy*, *83*(5), pp.614-624.

[80] Solanki, C.S., 2015. *Solar photovoltaics: fundamentals, technologies and applications*. PHI Learning Pvt. Ltd.

[81] Still, C.J., Riley, W.J., Biraud, S.C., Noone, D.C., Buenning, N.H., Randerson, J.T., Torn, M.S., Welker, J., White, J.W.C., Vachon, R. and Farquhar, G.D., 2009. Influence of clouds and diffuse radiation on ecosystem-atmosphere CO2 and CO18O exchanges. *Journal of Geophysical Research: Biogeosciences*, *114*(G1).

[82] Stull, R.B., 2012. *An introduction to boundary layer meteorology* (Vol. 13). Springer Science & Business Media.

[83] Styszko, K., Jaszczur, M., Teneta, J., Hassan, Q., Burzyńska, P., Marcinek, E., Łopian, N. and Samek, L., 2018. An analysis of the dust deposition on solar photovoltaic modules. *Environmental Science and Pollution Research*, pp.1-9.

[84] Šúri, M. and Cebecauer, T., 2010. SolarGIS: New web-based service offering solar radiation data and PV simulation tools for Europe, North Africa and Middle East. In *Proceedings of the International Conference on Solar Heating, Cooling and Buildings EUROSUN* (Vol. 28).

[85] Teo, H.G., Lee, P.S. and Hawlader, M.N.A., 2012. An active cooling system for photovoltaic modules. *Applied Energy*, *90* (1), pp.309-315.

[86] Tonui, J.K. and Tripanagnostopoulos, Y., 2007. Air-cooled PV/T solar collectors with low cost performance improvements. *Solar energy*, *81*(4), pp.498-511.

[87] Touati, F., Chowdhury, N.A., Benhmed, K., Gonzales, A.J.S.P., Al-Hitmi, M.A., Benammar, M., Gastli, A. and Ben-Brahim, L., 2017. Long-term performance analysis and power prediction of PV technology in the State of Qatar. *Renewable Energy*, *113*, pp.952-965.

[88] Traunmüller, W. and Steinmaurer, G., 2010, September. Solar irradiance forecasting, benchmarking of different techniques and applications of energy meteorology. In *Proceedings of the EuroSun 2010 conference*.

[89] Vasel, A. and Iakovidis, F., 2017. The effect of wind direction on the performance of solar PV plants. *Energy Conversion and Management*, *153*, pp.455-461.

[90] Vollmer, M., 2009. Newton's law of cooling revisited. *European Journal of Physics*, *30*(5), p.1063.

[91] Wan, C., Zhao, J., Song, Y., Xu, Z., Lin, J. and Hu, Z., 2015. Photovoltaic and solar power forecasting for smart grid energy management. *CSEE Journal of Power and Energy Systems*, *1*(4), pp.38-46.

[92] Wilson, J.D. and Yee, E., 2003. Calculation of winds disturbed by an array of fences. *Agricultural and forest meteorology*, *115*(1-2), pp.31-50.

[93] Wu, Y.Y., Wu, S.Y. and Xiao, L., 2017. Numerical study on convection heat transfer from inclined PV panel under windy environment. *Solar Energy*, *149*, pp.1-12.

[94] Xydis, G., 2013. The wind chill temperature effect on a large-scale PV plant—an exergy approach. *Progress in Photovoltaics: Research and Applications*, *21*(8), pp.1611-1624.

[95] Zaoui, F., Titaouine, A., Becherif, M., Emziane, M. and Aboubou, A., 2015. A combined experimental and simulation study on the effects of irradiance and temperature on photovoltaic modules. *Energy Procedia*, *75*, pp.373-380.

Appendix A

Table 3: Wind direction matches summary table.

	Southerly									Northerly									
Match #	Date (d.m.y h:m)	WD (°)	Wind Speed (m/s)	Amb Temp (°C)	RH (%)	Global PAR (J/m2)	Diffuse PAR (J/m2)	Panel Temperature (°C)	Electricity output (kWh)	Date (d.m.y h:m)	WD (°)	Wind Speed (m/s)	Amb Temp (°C)	RH (%)	Global PAR (J/m2)	Diffuse PAR (J/m2)	Panel Temperature (°C)	Electricity output (kWh)	S-N (Panel Temp)	S-N (Energy output)
1	02/07/2013 06:00	259.7	0.00	9.55	97.83	110160	111240	8.83	42	22/04/2014 07:00	25.3	0.00	8.93	99.40	99272	100667	8.81	50	0.02	-8
2	02/07/2013 07:00	209.2	0.25	11.32	97.85	307800	309960	11.07	122.5	22/04/2014 09:00	296.2	0.00	10.27	99.65	296283	297259	13.48	150	-2.41	-27.5
3	02/07/2013 07:00	209.2	0.25	11.32	97.85	307800	309960	11.07	122.5	24/06/2014 06:00	279.4	0.00	11.39	96.51	310505	283735	11.46	50	-0.39	72.5
4	05/07/2013 07:00	256.9	0.50	11.96	99.78	399600	400680	NA	134	03/04/2014 09:00	80.0	0.50	10.61	96.95	386353	387887	12.08	100		34
5	14/07/2013 06:00	263.9	0.00	12.78	96.73	176040	160920	NA	50.5	18/07/2013 06:00	78.6	0.00	12.75	97.13	156600	149040	13.42	40		10.5
6	14/07/2013 06:00	263.9	0.00	12.78	96.73	176040	160920	NA	50.5	28/08/2013 08:00	355.2	0.25	13.77	99.30	162000	163080	14.09	48		2.5
7	15/07/2013 06:00	237.3	0.00	9.09	97.38	222480	166320	NA	37.5	17/11/2013 12:00	26.7	0.00	8.44	100.00	242473	142072	10.54	59		-21.5
8	16/07/2013 13:00	217.6	0.76	30.58	45.73	3000000	919080	NA	964	17/07/2013 13:00	355.2	0.76	31.60	45.55	3300000	1000000	NA	885.5		78.5
9	21/07/2013 12:00	102.5	1.26	21.78	71.93	1800000	1800000	27.11	766.5	07/08/2013 12:00	70.2	1.51	21.55	69.28	2000000	1800000	NA	733		33.5
10	26/07/2013 06:00	237.3	0.00	12.47	98.63	163080	132840	12.58	26.5	18/07/2013 06:00	78.6	0.00	12.75	97.13	156600	149040	13.42	40	-0.84	-13.5
11	26/07/2013 06:00	237.3	0.00	12.47	98.63	163080	132840	12.58	26.5	28/08/2013 08:00	355.2	0.25	13.77	99.30	162000	163080	14.09	48	-1.51	-21.5
12	27/07/2013 06:00	235.9	0.00	8.32	97.13	99360	97200	8.84	35.5	22/04/2014 07:00	25.3	0.00	8.93	99.40	99272	100667	8.81	50	0.03	-14.5
13	29/07/2013 06:00	233.1	1.01	14.83	98.08	130680	110160	14.38	60.5	22/07/2013 07:00	70.2	1.01	15.75	98.50	105840	108000	15.73	30.5	-1.35	30
14	29/07/2013 10:00	249.9	2.27	21.68	80.88	1400000	1300000	23.58	587	25/08/2013 15:00	15.4	2.01	21.75	79.45	1300000	1300000	24.94	575.5	-1.36	11.5
15	30/07/2013 06:00	221.8	0.25	13.41	98.08	66960	68040	12.9	24	27/08/2013 07:00	57.6	0.25	12.32	98.80	77760	78840	12.4	30.5	0.5	-6.5
16	30/07/2013 11:00	238.7	0.00	16.59	97.48	783000	785160	17.85	154.5	24/06/2014 09:00	345.4	0.00	16.81	97.16	855945	837541	19.57	250	-1.72	-95.5
17	30/07/2013 12:00	259.7	0.00	17.28	98.00	496800	498960	19.92	324.5	22/08/2013 08:00	314.5	0.00	17.33	98.78	495720	484920	17.41	127	2.51	197.5
18	04/08/2013 06:00	214.8	0.50	13.67	99.15	76680	78840	NA	28.5	28/08/2013 07:00	342.6	0.50	13.19	99.30	63720	65880	13.23	20		8.5
19	13/08/2013 07:00	235.9	0.25	9.65	98.23	184680	185760	NA	67.5	01/04/2014 08:00	329.9	0.00	8.27	99.13	198405	199939	8.64	50		17.5
20	13/08/2013 07:00	235.9	0.25	9.65	98.23	184680	185760	NA	67.5	28/04/2014 08:00	26.7	0.25	9.28	98.80	165361	166895	9.62	50		17.5
21	13/08/2013 07:00	235.9	0.25	9.65	98.23	184680	185760	NA	67.5	24/05/2014 07:00	71.6	0.00	9.87	98.62	197569	198963	9.93	50		17.5
22	14/08/2013 07:00	238.7	0.00	9.62	98.68	293760	281880	NA	85	22/04/2014 08:00	331.3	0.00	9.26	99.48	281504	282898	9.78	50		35

23	14/08/2013 15:00	231.6	2.01	18.80	71.65	483840	486000	NA	273	10/07/2013 19:00	61.8	2.27	19.62	70.83	505440	503280	NA	111.5		161.5
24	17/08/2013 10:00	231.6	1.76	17.56	85.58	529200	519480	23.49	208	21/07/2013 08:00	74.4	1.76	16.92	83.33	496800	498960	18.47	146.5	5.02	61.5
25	17/08/2013 11:00	256.9	2.52	18.31	80.93	837000	828360	20.35	241.5	24/08/2013 14:00	320.1	2.77	18.37	79.23	848880	851040	19.92	260.5	0.43	-19
26	19/08/2013 07:00	258.3	0.50	11.59	97.90	182520	184680	10.83	76.5	29/05/2014 07:00	39.3	0.76	11.81	99.87	168010	169404	12.27	50	-1.44	26.5
27	01/09/2013 08:00	255.5	0.50	9.10	95.45	438480	435240	8.55	317	25/03/2014 11:00	1.4	0.76	8.28	93.98	443519	440451	9.45	100	-0.9	217
28	03/09/2013 08:00	252.7	0.00	12.37	99.15	412560	407160	13.46	525	27/08/2013 09:00	49.1	0.25	13.23	99.25	407160	409320	13.78	165.5	-0.32	359.5
29	15/10/2013 13:00	226.7	0.46	12.46	90.19	623160	613440	17.67	164	17/06/2014 07:00	43.5	0.76	12.15	89.53	636486	539305	13.4	100	4.27	64
30	15/10/2013 14:00	242.2	0.17	12.23	89.17	514080	515160	15.27	163.5	26/05/2014 14:00	81.4	0.25	12.09	88.32	496362	498035	13.44	150	1.83	13.5
31	16/10/2013 09:00	104.6	0.29	7.99	100.00	50760	51840	8	14	07/08/2013 06:00	60.4	0.00	7.41	97.63	51840	52920	NA	26		-12
32	16/10/2013 09:00	104.6	0.29	7.99	100.00	50760	51840	8	14	15/10/2013 08:00	291.8	0.04	6.60	99.98	66960	68040	5.39	38.5	2.61	-24.5
33	16/10/2013 09:00	104.6	0.29	7.99	100.00	50760	51840	8	14	27/11/2013 10:00	297.6	0.00	7.96	97.95	77027	47412	9.26	15	-1.26	-1
34	18/10/2013 10:00	124.7	0.59	12.98	99.90	252720	254880	13.43	106.5	27/08/2013 08:00	54.8	0.50	12.21	99.13	253800	255960	12.57	97.5	0.86	9
35	31/10/2013 09:00	236.6	0.04	9.90	98.75	116640	118800	11.05	45.5	22/04/2014 07:00	25.3	0.00	8.93	99.40	99272	100667	8.81	50	2.24	-4.5
36	31/10/2013 10:00	224.9	0.34	11.07	97.99	321840	320760	12.07	95	22/04/2014 09:00	296.2	0.00	10.27	99.65	296283	297259	13.48	150	-1.41	-55
37	31/10/2013 10:00	224.9	0.34	11.07	97.99	321840	320760	12.07	95	24/06/2014 06:00	279.4	0.00	11.39	96.51	310505	283735	11.46	50	0.61	45
38	06/11/2013 10:00	202.2	0.00	9.67	99.73	233504	136940	11.59	35.5	17/11/2013 12:00	26.7	0.00	8.44	100.00	242473	142072	10.54	59	1.05	-23.5
39	08/11/2013 14:00	238.7	0.00	8.27	98.45	145411	86538	8.18	40.5	17/11/2013 11:00	329.9	0.00	8.05	99.98	162798	96486	9.57	43	-1.39	-2.5
40	11/11/2013 10:00	199.4	1.76	10.30	98.98	77027	47412	11.49	17	13/10/2013 10:00	328.7	1.68	10.44	98.65	50760	51840	10.68	36.5	0.81	-19.5
41	16/11/2013 15:00	244.3	0.00	7.14	98.45	180300	106500	7.71	36	18/11/2013 10:00	276.6	0.00	7.12	100.00	145411	86538	10	55	-2.29	-19
42	16/11/2013 15:00	244.3	0.00	7.14	98.45	180300	106500	7.71	36	28/11/2013 10:00	328.5	0.00	7.80	97.08	145411	86538	9.35	41.5	-1.64	-5.5
43	09/12/2013 10:00	237.3	0.25	7.51	99.95	119550	71742	9.7	28.5	17/11/2013 10:00	278.0	0.00	7.12	99.93	119550	71742	8.78	32.5	0.92	-4
44	09/12/2013 12:00	233.1	0.50	9.50	96.08	525038	303740	11.17	107	28/11/2013 13:00	2.8	0.50	8.77	94.15	554731	320729	9.43	91.5	1.74	15.5
45	12/12/2013 10:00	196.5	0.25	7.19	99.73	162798	96486	8.42	66.5	18/11/2013 10:00	276.6	0.00	7.12	100.00	145411	86538	10	55	-1.58	11.5
46	12/12/2013 10:00	196.5	0.25	7.19	99.73	162798	96486	8.42	66.5	28/11/2013 10:00	328.5	0.00	7.80	97.08	145411	86538	9.35	41.5	-0.93	25
47	19/12/2013 11:00	212.0	0.25	4.96	92.68	418397	242726	12.16	425.5	15/11/2013 10:00	325.7	0.00	4.17	92.83	456769	264680	16.09	468	-3.93	-42.5
48	19/12/2013 12:00	233.1	1.51	6.50	88.53	505387	292497	13.64	623.5	25/11/2013 13:00	21.1	1.26	6.05	87.38	505387	292497	7.35	130	6.29	493.5
49	04/01/2014 13:00	226.0	0.00	6.72	98.85	154625	156019	6.51	100	12/07/2013 06:00	33.7	0.00	6.30	97.55	157680	137160	NA	36		64
50	13/01/2014 10:00	216.2	0.00	3.79	97.68	398902	171914	9.84	100	22/11/2013 10:00	22.5	0.25	2.38	98.88	333759	194300	9.77	272.5	0.07	-172.5
51	04/02/2014 15:00	178.3	2.27	7.44	83.48	635371	346895	13.23	150	22/11/2013 14:00	23.9	2.01	7.25	84.35	604800	349376	11.62	485	1.61	-335

52	18/02/2014 11:00	219.0	0.76	8.11	95.98	458158	436547	11.58	50	25/03/2014 11:00	1.4	0.76	8.28	93.98	443519	440451	9.45	100	2.13	-50
53	02/03/2014 16:00	196.5	3.02	8.13	95.85	214161	214579	8.39	100	20/04/2014 10:00	54.8	3.02	8.76	94.08	225175	226709	9.15	50	-0.76	50
54	05/03/2014 12:00	221.8	0.25	9.28	88.70	999695	985473	15.55	500	11/04/2014 09:00	296.2	0.25	9.48	87.23	920221	893451	NA	300.49		199.51
55	13/03/2014 18:00	113.7	0.00	10.69	96.58	131341	125066	5.68	200	07/08/2013 07:00	59.0	0.00	11.56	98.35	137160	137160	NA	43		157
56	17/03/2014 09:00	247.1	0.00	8.07	99.33	341318	342852	10.71	50	03/04/2014 08:00	43.5	0.25	9.79	97.88	341737	340342	9.62	50	1.09	0
57	21/03/2014 09:00	256.9	1.26	7.05	89.88	1100000	210675	14.59	350	14/04/2014 08:00	283.6	1.51	7.99	91.13	1100000	225733	NA	163.04		186.96
58	22/04/2014 16:00	212.0	1.26	14.37	82.95	983242	897076	19.63	450	27/05/2014 13:00	39.3	1.51	15.81	85.01	917711	918827	18.33	400	1.3	50
59	22/04/2014 19:00	192.3	1.01	12.14	86.78	81844	82959	13.82	100	25/08/2013 08:00	329.9	1.01	13.68	88.05	85320	87480	14.03	18	-0.21	82
60	23/04/2014 13:00	178.3	1.76	14.32	80.55	497059	491621	20.8	450	27/05/2014 14:00	32.3	1.76	14.04	82.19	525363	526617	16.56	250	4.24	200
61	23/04/2014 15:00	192.3	1.51	12.57	87.10	305346	306740	14.68	50	03/04/2014 16:00	37.9	1.51	13.64	87.25	299351	300745	15.47	100	-0.79	-50
62	23/04/2014 19:00	217.6	0.00	10.69	95.65	87839	88536	11.02	50	26/05/2014 18:00	23.9	0.00	11.61	94.55	114749	115864	11.98	50	-0.96	0
63	01/05/2014 10:00	213.4	0.00	12.00	98.30	707455	707594	14.87	150	05/07/2013 08:00	275.2	0.25	13.32	99.68	749520	741960	NA	268		-118
64	08/05/2014 07:00	237.3	1.01	10.07	94.00	205377	207050	10.17	50	27/05/2014 17:00	5.6	1.01	11.70	94.38	215276	216391	12.04	50	-1.87	0
65	26/05/2014 07:00	103.9	0.00	8.32	97.36	355679	356098	8.59	50	03/04/2014 08:00	43.5	0.25	9.79	97.88	341737	340342	9.62	50	-1.03	0
66	04/06/2014 07:00	244.3	0.00	10.79	98.07	283595	284990	11.25	50	22/04/2014 09:00	296.2	0.00	10.27	99.65	296283	297259	13.48	150	-2.23	-100
67	04/06/2014 07:00	244.3	0.00	10.79	98.07	283595	284990	11.25	50	24/06/2014 06:00	279.4	0.00	11.39	96.51	310505	283735	11.46	50	-0.21	0
68	09/06/2014 13:00	249.9	2.01	23.85	69.64	2100000	1100000	33.69	850	18/06/2014 13:00	53.3	2.01	22.39	69.26	2200000	1000000	32.39	850	1.3	0
69	22/06/2014 15:00	188.1	0.76	26.72	50.80	2000000	1100000	47.68	800	12/07/2013 17:00	47.7	0.76	27.64	48.08	1800000	1100000	NA	490.5		309.5
70	26/06/2014 19:00	219.0	0.50	14.03	84.81	79892	80868	14.51	50	15/06/2014 20:00	67.4	0.76	15.68	85.96	83517	84632	16.64	50	-2.13	0

842

843